CAMBRIDGE
UNIVERSITY PRESS

Article

Tetrahedrite-(Cu), $Cu_{12}Sb_4S_{13}$, from Bankov near Košice, Slovak Republic: a new member of the tetrahedrite group

Jiří Sejkora[1,2] (iD), Cristian Biagioni[3,4] (iD), Martin Števko[2,1] (iD), Silvia Musetti[3] and Dušan Peterec[5]

[1]Department of Mineralogy and Petrology, National Museum, Cirkusová 1740, 193 00, Praha 9, Czech Republic; [2]Earth Science Institute, Slovak Academy of Sciences, Dúbravská cesta 9, 840 05 Bratislava, Slovak Republic; [3]Dipartimento di Scienze della Terra, Università di Pisa, Via Santa Maria 53, 56126 Pisa, Italy; [4]Centro per l'Integrazione della Strumentazione Scientifica dell'Università di Pisa, Pisa, Italy; and [5]Rovníková 8, 040 12 Košice, Slovak Republic

Abstract

Tetrahedrite-(Cu), $Cu_{12}Sb_4S_{13}$, has been approved as a new mineral species (IMA2022–078) from the Bankov magnesite deposit near Košice, Slovak Republic where it occurs as anhedral grains, up to 0.4 mm across, associated with skinnerite, chalcostibite, famatinite, tetrahedrite-(Fe) and zoned aggregates of tennantite-(Cu) to tennantite-(Fe). Tetrahedrite-(Cu) is steel-grey, with a metallic lustre. Mohs hardness is *ca.* 3½–4 and calculated density is 5.029 g.cm^{-3}. In reflected light, tetrahedrite-(Cu) is isotropic and grey with a bluish shade. Reflectance data for the four COM wavelengths in air are [λ (nm): R (%)]: 470: 31.1; 546: 30.1; 589: 29.9; and 650: 28.1. The empirical formula, based on electron-microprobe data (mean of 17 spot analyses), is $Cu_{11.42}Zn_{0.26}Fe_{0.19}(Sb_{4.06}As_{0.08})_{\Sigma4.14}S_{12.99}$. The ideal formula is $Cu_6(Cu_4Cu_2)Sb_4S_{13}$, which requires (in wt.%) Cu 45.76, Sb 29.23 and S 25.01, total 100.00. Tetrahedrite-(Cu) is cubic, $I\bar{4}3m$, with unit-cell parameters $a = 10.3296(15)$ Å, $V = 1102.2(5)$ Å^3 and $Z = 2$. Its crystal structure was refined by single-crystal X-ray diffraction data to a final $R_1 = 0.0347$ on the basis of 261 unique reflections with $F_o > 4\sigma(F_o)$ and 22 refined parameters. Tetrahedrite-(Cu) is isotypic with other tetrahedrite-group minerals. Previous findings of tetrahedrite-(Cu) are reported and some nomenclature issues, related to the Fe and Cu oxidation states, are discussed. At the Bankov deposit, tetrahedrite-(Cu) is related to hydrothermal, most probably Alpine, solutions strongly enriched in Cu, Sb and S.

Introduction

Tetrahedrite-group minerals are characterised by the general structural formula $^{M(2)}A_6{}^{M(1)}(B_4C_2)^{X(3)}D_4{}^{S(1)}Y_{12}{}^{S(2)}Z$, where the capital letters indicate several chemical constituents. Among the different species, the most common belong to the tetrahedrite and tennantite series and are characterised by A and B = Cu$^+$, D = Sb^{3+} or As^{3+}, and Y and Z = S^{2-}. Different C constituents, usually represented by divalent transition elements, identify the species belonging to these series (Biagioni *et al.*, 2020a).

The name 'tetrahedrite' was introduced by Haidinger (1845) in agreement with the common tetrahedral form of its crystals. Previously, tetrahedrite was known with different names, for instance fahlerz, fahlerts, weissgiltigerz, grey ore, or panabase. Haidinger (1845) reported the occurrence of Fe and Zn in tetrahedrite. Indeed, these two constituents are its most common divalent cations (e.g. Johnson *et al.*, 1986; George *et al.*, 2017).

Biagioni *et al.* (2020a) renamed these species as tetrahedrite-(Fe) and tetrahedrite-(Zn). Moreover, since the publication of the nomenclature of tetrahedrite-group minerals (Biagioni *et al.*,

2020a), four other species belonging to the tetrahedrite series have been approved by the Commission on New Minerals, Nomenclature and Classification of the International Mineralogical Association (IMA-CNMNC), i.e. tetrahedrite-(Hg) (Biagioni *et al.*, 2020b), tetrahedrite-(Mn) (Momma *et al.*, 2022), tetrahedrite-(Ni) (Wang *et al.*, 2023) and tetrahedrite-(Cd) (Sejkora *et al.*, 2023). Other potential end-member compositions are known in literature. Among them, Cu-dominant compositions corresponding to ideal $Cu_{12}Sb_4S_{13}$ have been reported, for instance from Greece, France and the Czech Republic (Cesbron *et al.*, 1985; Repstock *et al.*, 2015; Voudouris *et al.*, 2022; Sejkora *et al.*, 2023). 'Unsubstituted' tetrahedrite–tennantite (i.e. without metals other than Cu and Ag) is also known from synthetic samples (Makovicky *et al.*, 2005); the apparent excess of negative charges could be compensated by the presence of formally divalent Cu (Pattrick *et al.*, 1993). According to Makovicky and Skinner (1979), synthetic tetrahedrite $Cu_{12+x}Sb_4S_{13}$ (*x* varies continuously between < 0.1 and 1.9) exsolves, below 120°C, to a composition close to $Cu_{12}Sb_4S_{13}$ ($a = 10.32$ Å) and to a Cu-excess composition, close to $Cu_{14-x}Sb_4S_{13}$ (*x* approximately equal to 0.2; $a = 10.45$ Å). The Cu-excess variety could be more common than previously thought, but, as stressed by Lind and Makovicky (1982), during electron-microprobe analysis a 'loss' of Cu over 12 atoms per formula unit (apfu) was observed, both in synthetic as well as in natural samples of tetrahedrite and tennantite.

A new study of samples from the Slovak magnesite deposit Bankov near Košice (Peterec *et al.*, 1990) resulted in the description of the new mineral species tetrahedrite-(Cu). The new mineral and its name have been approved by the IMA–CNMNC, under the voting number IMA2022-078 (Sejkora *et al.*, 2022). Tetrahedrite-(Cu) is named after its chemical composition, in agreement with the nomenclature of the tetrahedrite group (Biagioni *et al.*, 2020a). Its mineral symbol, in accord with Warr (2021), is Ttr-Cu. Holotype material of tetrahedrite-(Cu) is deposited in the collections of the Department of Mineralogy and Petrology, National Museum in Prague, Cirkusová 1740, 193 00 Praha 9, Czech Republic under the catalogue number P1P 27/2022 and in the collections of the Museo di Storia Naturale of the Università di Pisa, Via Roma 79, Calci (PI), under catalogue number 20017.

This work reports a description of this new mineral species, its position in the tetrahedrite group, and some crystal-chemical and nomenclature issues are discussed.

Occurrence and physical properties

Occurrence

Tetrahedrite-(Cu) was found at the stope K 401, in the 4th horizon of the Medvedza magnesite body, Bankov magnesite deposit near Košice (GPS coordinates: 48°44'8.06''N, 21°13'40.10''E), Košice Co., Košice Region, Slovak Republic. Hydrothermal-metasomatic bodies of magnesite at the Bankov deposit are hosted in Carboniferous shales and phyllites belonging to the Gemeric tectonic unit (Grecula *et al.*, 1995). Here an interesting hydrothermal ore mineralisation, represented mostly by Cu sulfosalts (skinnerite, chalcostibite and various minerals of the tetrahedrite group), is developed in a small scale on younger fractures in the Medvedza magnesite body in the form of crystalline crusts and fillings (Peterec *et al.*, 1990). Tetrahedrite-(Cu) is associated with skinnerite, chalcostibite, famatinite, tetrahedrite-(Fe), zoned aggregates of tennantite-(Cu) to tennantite-(Fe) and minor chalcopyrite and marcasite. This unusual association of Cu sulfosalts has no other equivalent in the whole Western Carpathians and it is related to hydrothermal, most probably Alpine solutions strongly enriched in Cu, Sb and S and later stages of crystallisation also rich in As as well as minor amounts of Ge. The primary ore mineralisation is locally replaced by younger supergene minerals including chalcocite, native copper, malachite and azurite.

Physical and optical properties

Tetrahedrite-(Cu) forms anhedral grains up to 200×400 μm (Fig. 1). It is steel-grey in colour, with a black streak and metallic lustre. Mohs hardness was not measured, owing to the small size of the studied grain and the intimate association of other sulfides, but it should be close to 3½–4, in agreement with other members of the tetrahedrite group. Tetrahedrite-(Cu) is brittle, with a conchoidal fracture and an indistinct cleavage. Due to the small size of the studied grains and their admixure with other sulfides, density was not measured; on the basis of the empirical formula and the single crystal X-ray diffraction data, the calculated density is 5.029 g·cm^{-3}.

In reflected light, tetrahedrite-(Cu) is isotropic and grey, with a bluish shade (Fig. 2). Internal reflections were not observed. Reflectance values measured in air on the holotype sample using a spectrophotometer MSP400 Tidas with Leica microscope,
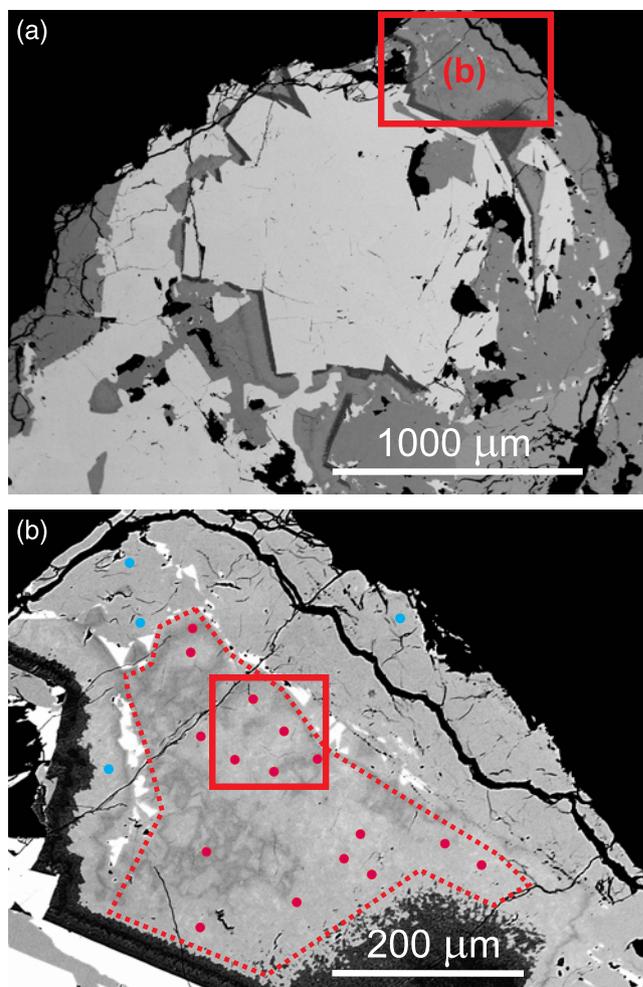

Figure 1. Back-scattered electron images of tetrahedrite-(Cu), associated with chalcostibite (white) and tennantite-(Fe) (dark grey) (a). Inset (b) shows details of tetrahedrite-(Cu): red points correspond to tetrahedrite-(Cu), observed zonality reflects Cu–Zn–Fe and Sb–As substitutions; the rest of the grey aggregate (marked by blue points) is Fe-richer tetrahedrite-(Cu) with contents 0.89–0.99 apfu Fe and without Zn and As. The grain used for single-crystal X-ray diffraction study was extracted from the area of the red box. Holotype sample, catalogue number P1P 27/2022.
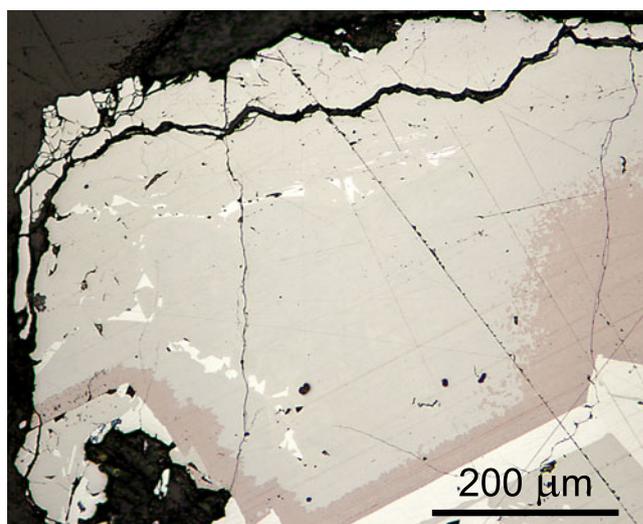

Figure 2. Reflected-light photo of grey tetrahedrite-(Cu) associated with chalcostibite (white) and tennantite-(Fe) (pink-brownish grey). Holotype sample, catalogue number P1P 27/2022.

Table 1. Reflectance values (%) for tetrahedrite-(Cu).*

λ (nm)	R (%)	λ (nm)	R (%)
400	32.7	560	30.0
420	32.4	580	30.0
440	32.0	**589**	**29.9**
460	31.5	600	29.7
470	**31.1**	620	29.2
480	30.9	640	28.5
500	30.5	**650**	**28.1**
520	30.2	660	27.6
540	30.0	680	26.6
546	**30.1**	700	25.7

* The reference wavelengths required by the Commission on Ore Mineralogy (COM) are given in bold.

Table 2. Compositional data (wt.%) from electron microprobe analysis of tetrahedrite-(Cu) ($n = 17$).

Constituent	Mean	Range	(σ)
Cu	43.24	41.79–44.54	0.93
Fe	0.63	0.40–1.18	0.23
Zn	1.00	0.51–2.01	0.41
As	0.34	0.06–1.41	0.43
Sb	29.41	27.49–30.32	0.75
S	24.80	24.50–25.28	0.18
Total	99.42	99.07–99.94	0.27

(σ) – estimated standard deviation.

with a 20× objective, are given in Table 1 and shown in Fig. 3, where the reflectance curve for tetrahedrite-(Cu) is compared with published data for related tetrahedrite-group minerals.

Chemical composition

Quantitative chemical analyses were carried out using a Cameca SX 100 electron microprobe (National Museum of Prague, Czech Republic) and the following experimental conditions: wavelength-dispersive spectroscopy mode, accelerating voltage = 25 kV, beam current = 20 nA, beam diameter = 1 μm. Standards (element, emission line) were: chalcopyrite (Cu$K\alpha$, S$K\alpha$), pyrite (Fe$K\alpha$), ZnS (Zn$K\alpha$), NiAs (As$L\beta$) and Sb$_2$S$_3$ (Sb$L\alpha$). The contents of other sought elements with $Z > 8$ (Ag, Au, Bi, Cd, Co, Ga, Ge, Hg, In, Mn, Cl, Ni, Pb, Se, Sn, Te and Tl) were below detection limits. Matrix correction by the PAP procedure (Pouchou and Pichoir, 1985) was applied to the data. Electron back-scattered images showed that tetrahedrite-(Cu) is slightly zoned due to Cu–Fe–Zn and As–Sb substitutions. Results are given in Table 2.

X-ray diffraction data

Single-crystal X-ray diffraction intensity data were collected on an anhedral grain of tetrahedrite-(Cu), 60×40×30 μm in size, using a
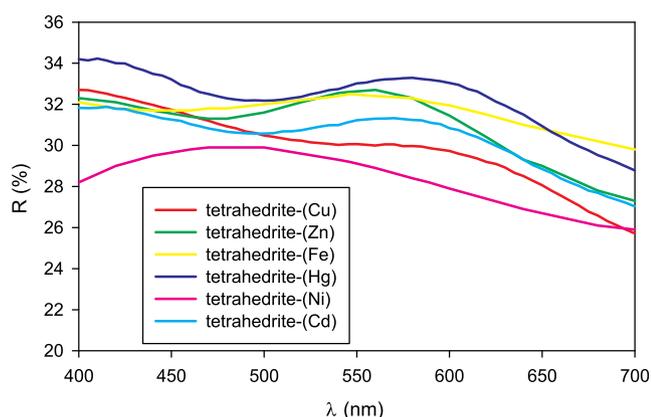

Figure 3. Reflectance curves for tetrahedrite-(Cu) from the Bankov deposit, compared with published data for other tetrahedrite-series minerals: tetrahedrite-(Cu) (this paper); tetrahedrite-(Zn), Fresney d´Oisans, Isère, France (Criddle and Stanley, 1993); tetrahedrite-(Fe), Frigido mine, Massa, Tuscany, Italy (Criddle and Stanley, 1993); tetrahedrite-(Hg), Buca della Vena mine, Apuan Alps, Tuscany, Italy (Biagioni et al., 2020b), tetrahedrite-(Ni), Luobusa, Tibet, China (Wang et al., 2023); tetrahedrite-(Cd), Radětice near Příbram, Czech Republic (Sejkora et al., 2023).

Bruker D8 Venture four-circle diffractometer equipped with an air-cooled Photon III detector, and microfocus Mo$K\alpha$ radiation (Centro per l'Integrazione della Strumentazione Scientifica dell'Università di Pisa, Pisa, Italy). The detector-to-crystal distance was set to 38 mm. Data were collected using φ and ω scan modes, in 0.5° slices, with an exposure time of 45 s per frame. A total of 1496 frames were collected. The frames were integrated with the Bruker *SAINT* software package using a narrow-frame algorithm. Data were corrected for Lorentz-polarisation, absorption and background. Unit-cell parameters, refined on the basis of the XYZ centroids of 622 reflections above 20 σI with $11.17 < 2\theta < 45.81°$, are $a = 10.3296(15)$ Å, $V = 1102.2(8)$ Å^3 and space group $I\bar{4}3m$. The crystal structure of tetrahedrite-(Cu) was refined using *Shelxl*-2018 (Sheldrick, 2015) starting from the atomic coordinates of Johnson and Burnham (1985). The occurrence of a racemic twin was modelled. The M(2) site was found to be split into two sub-positions, M(2a) and M(2b). The following neutral scattering curves, taken from the *International Tables for Crystallography* (Wilson, 1992) were used: Cu vs □ at M(2a); Cu vs □ at M(2b); Cu vs Fe at M(1); As vs Sb at X(3); and S vs □ at S(1) and S(2) sites (where □ = vacancy). Unconstrained refinement of the site occupancy at the M(2a) and M(2b) positions results in a total Cu content of $0.51(2) + 0.242$ $(9) \times 2 = 1.008$ Cu atoms, indicating that no detectable Cu-excess occurs in the sample studied. Consequently, the sum of the site occupancy factors at M(2a) and M(2b) was constrained to one. The X(3) site was found fully occupied by Sb, whereas the S(1) and S(2) sites were found fully occupied by S. For these reasons, the site occupancies at these positions were fixed to one. The anisotropic structural model converged to $R_1 = 0.0347$ for 261 reflections with $F_o > 4\sigma(F_o)$ and 22 refined parameters. Details of the data collection and crystal structure refinement are reported in Table 3. Fractional atomic coordinates and equivalent isotropic displacement parameters are reported in Table 4, whereas Table 5 reports selected bond distances and Table 6 the weighted bond-valence balance calculated according to the bond parameters of Brese and O'Keeffe (1991). The crystallographic information file has been deposited with the Principal Editor of *Mineralogical Magazine* and is available as Supplementary material (see below).

Powder X-ray diffraction data were not collected, owing to the small size of the available grains and their admixture with other phases. Table 7 reports the calculated powder X-ray diffraction pattern.

Results and discussions

Chemical formula

As discussed in previous papers (e.g. Sejkora et al., 2021), there are different approaches to recalculating the chemical formulae

Table 3. Summary of data collection conditions and refinement parameters for tetrahedrite-(Cu).

Crystal data	
Crystal size (mm)	$0.060 \times 0.040 \times 0.030$
Cell setting, space group	Cubic, $I\bar{4}3m$
a (Å)	10.3296(15)
V (Å³)	1102.2(5)
Z	2
Data collection and refinement	
Radiation, wavelength (Å)	Mo$K\alpha$, $\lambda = 0.71073$
Temperature (K)	293(2)
$2\theta_{max}$ (°)	55.96
Measured reflections	41801
Unique reflections	280
Reflections with $F_o > 4\sigma(F_o)$	261
R_{int}	0.0845
$R\sigma$	0.0395
Range of h, k, l	$-7 \leq h \leq 7$
	$-9 \leq k \leq 9$
	$-13 \leq l \leq 13$
R [$F_o > 4\sigma(F_o)$]	0.0347
R (all data)	0.0422
wR (on F_o^2)[1]	0.0643
Goof	1.119
Absolute structure parameter[2]	$-0.16(10)$
Number of least-squares parameters	22
Maximum and	0.50 [at 1.58 Å from M(2a)]
minimum residual peak (e^- Å^{-3})	-0.54 [at 0.85 Å from X(3)]

[1] $w = 1/[\sigma^2(F_o^2)+(0.0262P)^2]$; [2]Flack (1983).

Table 5. Selected bond distances (in Å) for tetrahedrite-(Cu).

M(1)–S(1)	×4	2.316(2)
M(2a)–S(2)		2.254(7)
M(2a)– S(1)	×2	2.251(5)
M(2b)–S(2)		2.299(11)
M(2b)–S(1)	×2	2.304(8)
X(3)–S(1)	×3	2.440(4)

Table 6. Weighted bond-valence sums (in valence unit) in tetrahedrite-(Cu).

Site	M(1)	M(2a)	M(2b)	X(3)	Σanions	Theor.
S(1)	$0.32^{2\times\rightarrow\times4\downarrow}$	$0.18^{\times2\downarrow}$	$0.07^{2\times\rightarrow\times2\downarrow}$	$1.03^{\times3\downarrow}$	1.99	2.00
S(2)		$0.18^{6\times\rightarrow}$	$0.08^{12\times\rightarrow}$		2.04	2.00
Σcations	1.28	0.54	0.22	3.09		
Theor.	1.33	0.51	0.22	3.00		

of tetrahedrite-group minerals. The two better ones normalise the number of atoms on the basis of $\Sigma Me = 16$ apfu or on the basis of $(As + Sb + Te + Bi) = 4$ apfu. The former approach assumes that no vacancies occur at the M(2), M(1) and X(3) sites, whereas the latter is mainly based on the results discussed by Johnson *et al.* (1986) who revealed that negligible variations in the ideal number of X(3) atoms usually occurs.

The first approach gives the chemical formula $Cu_{11.42}Zn_{0.26}Fe_{0.19}(Sb_{4.06}As_{0.08})_{\Sigma4.14}S_{12.99}$, whereas the other normalisation strategy corresponds to the formula $Cu_{11.06}Zn_{0.25}Fe_{0.18}(Sb_{3.93}As_{0.07})_{\Sigma4.00}S_{12.57}$. The simplified formula of tetrahedrite-(Cu) is $Cu_6Cu_4(Cu^{2+},Zn,Fe)_2(Sb,As)_4S_{13}$, corresponding to the end-member formula $Cu_6(Cu_4Cu_2)Sb_4S_{13}$. It corresponds to (in wt.%) Cu 45.76, Sb 29.23, S 25.01, total 100.00.

Crystal structure description

The crystal structure of tetrahedrite-(Cu) agrees with the general features of the members of the tetrahedrite isotypic group. The M(2) site is split into two sub-positions, namely M(2a) and M(2b). The former has a triangular planar coordination, whereas the latter has a flat trigonal pyramidal coordination. This feature agrees with previous studies (e.g. Andreasen *et al.*, 2008; Welch *et al.*, 2018). Average bond distances are 2.253 and 2.302 Å for M(2a) and M(2b), respectively. Copper was hosted at both sub-positions.

The tetrahedrally coordinated M(1) site has an average bond distance of 2.316 Å, shorter than that observed in mixed (Cu,Zn,Fe) tetrahedral sites in tetrahedrite-group minerals (e.g. Wuensch, 1964; Wuensch *et al.*, 1966) and similar to that reported by Makovicky and Skinner (1979) for synthetic $Cu_{12.3}Sb_4S_{13}$, i.e. 2.311(4) Å. On the basis of the electron microprobe data, this site should have the occupancy ($Cu_{0.92}Zn_{0.05}Fe_{0.03}$), corresponding to 28.96 electrons per site, to be compared with a refined mean atomic number of ~29 electrons. Taking into account the low Fe content, it is possible that Fe occurs as Fe^{3+} (e.g. Makovicky *et al.*, 2003), and the actual population may be described as ($Cu^+_{0.70}Cu^{2+}_{0.22}Zn_{0.05}Fe^{3+}_{0.03}$). Using the bond parameters of Brese and O'Keeffe (1991), the following ideal distances can be calculated for tetrahedral coordination: Cu^+ 2.373 Å; Cu^{2+} 2.116 Å; Zn^{2+} 2.346 Å; and Fe^{3+} 2.266 Å. The proposed site occupancy would correspond to a calculated $<M(1)-S(1)>$ distance of 2.312 Å, to be compared with an observed value of 2.316 Å.

The X(3) site has an average bond distance of 2.439 Å and a refined site occupancy factor indicating a full occupancy by Sb, in agreement with electron microprobe data that indicate only a very minor replacement of Sb by As, with an As/(Sb+As) atomic ratio of 0.02.

The weighted bond-valence calculations are in Table 6, obtained using the bond-valence parameters of Brese and O'Keeffe (1991), assuming the simplified structural formula $^{M(2)}Cu_{6.00}{}^{M(1)}[Cu_4(Cu_{1.5}Zn_{0.30}Fe_{0.20})]^{X(3)}Sb_4S_{13}$.

Relationship between unit-cell parameter and chemical composition

The unit-cell parameter of tetrahedrite-(Cu) from Bankov [i.e. $a = 10.3296(15)$ Å] is identical with that of synthetic stoichiometric $Cu_{12}Sb_4S_{13}$ [$a = 10.3293(6)$ Å] described by Pfitzner *et al.* (1997) and agrees with data of synthetic $Cu_{12.3}Sb_4S_{13}$ studied by

Table 4. Sites, fractional atom coordinates, equivalent isotropic displacement parameters (Å²), and refined (obs) and calculated (calc) mean atomic numbers for tetrahedrite-(Cu).

Site	x/a	y/b	z/c	U_{eq}	SREF$_{obs}$		SREF$_{calc}$
M(2a)	0.2183(7)	0	0	0.024(4)	14.9(5) ⎫	29.0(10)	29.0
M(2b)	0.2177(10)	0.9674(16)	$-0.9674(16)$	0.024(4)	14.1(5) ⎬		
M(1)	¼	½	0	0.0254(10)		29(4)	28.9
X(3)	0.26853(9)	0.26853(9)	0.26853(9)	0.0203(4)		51.0	51.0
S(1)	0.1154(3)	0.1154(3)	0.3627(3)	0.0189(8)		16.0	16.0
S(2)	0	0	0	0.025(3)		16.0	16.0

Table 7. Calculated X-ray powder diffraction data for tetrahedrite-(Cu).*

I_{calc}	d_{calc}	$h\,k\,l$	I_{calc}	d_{calc}	$h\,k\,l$
1	7.304	1 1 0	6	2.026	4 3 1
4	5.165	2 0 0	7	1.886	5 2 1
3	4.217	2 1 1	**40**	**1.826**	**4 4 0**
9	**3.652**	**2 2 0**	3	1.772	4 3 3
100	**2.982**	**2 2 2**	1	1.722	4 4 2
7	2.761	3 2 1	2	1.676	5 3 2
21	**2.582**	**4 0 0**	6	1.676	6 1 1
1	2.435	3 3 0	1	1.633	6 2 0
7	2.435	4 1 1	1	1.594	5 4 1
2	2.310	4 2 0	**19**	**1.557**	**6 2 2**
2	2.202	3 3 2	2	1.523	6 3 1
2	2.109	4 2 2	2	1.491	4 4 4
2	2.026	5 1 0			

*Intensity and d_{hkl} were calculated using the software *PowderCell*2.3 (Kraus and Nolze, 1996) on the basis of the structural model given in Table 4. Only reflections with $I_{calc} > 1$ are listed. The five strongest reflections are given in bold.

Makovicky and Skinner (1979), where $a = 10.323(1)$ Å. No evidence of exsolution of Cu-poor and Cu-rich domains within tetrahedrite-(Cu) were observed. On the contrary, the synthetic sample studied by Di Benedetto et al. (2005) gave a unit-cell parameter of $a = 10.383(5)$ Å.

The relationships between chemistry and unit-cell parameter proposed by Johnson et al. (1987) apparently does not correctly describe the behaviour of tetrahedrite-(Cu). Indeed, the calculated a parameter is 10.37 Å, assuming the occurrence of ≈ 1.5 Cu^{2+} apfu. A better fit is obtained using the relationship proposed by Charlat and Lévy (1975), obtaining a calculated a value of 10.34 Å.

Comparison between tetrahedrite-(Cu) and previous findings of Cu-rich tetrahedrites

The occurrence of tetrahedrite samples having formally divalent Cu as the dominating C-cation has been reported from some other occurrences. For instance, Cesbron et al. (1985) reported chemical data for sample 2 from Chizeuil, France which corresponds to the empirical formula $Cu_6[Cu_4(Cu_{0.74}Fe_{0.71}Zn_{0.42})_{\Sigma1.87}]$ $(Sb_{2.58}As_{1.53}Bi_{0.01})_{\Sigma4.12}S_{13.46}$. Repstock et al. (2015) documented Cu contents up to 11.12 apfu (analysis 15) in specimens from the Pefka deposit, Northeastern Greece, corresponding to the empirical formula $Cu_6[Cu_4(Cu_{1.12}Zn_{0.88}Fe_{0.09})_{\Sigma2.09}](Sb_{2.09}As_{1.81}Te_{0.14})_{\Sigma4.04}S_{13.30}$. Voudouris et al. (2022) described a potential Cd–Mn bearing 'tetrahedrite-(Cu)' with 10.94 apfu Cu as inclusions up to 10 μm across within galena from St Philippos, Greece. The occurrence of Pb- and Cd-bearing tetrahedrite-(Cu) in association with tetrahedrite-(Cd) was mentioned by Sejkora et al. (2023) at the Radětice deposit near Příbram, Czech Republic.

Natural members of the tetrahedrite series are usually characterised by the formula $Cu_6(Cu_4Me_2)Sb_4S_{13}$, where Me is commonly Fe and Zn. However, synthetic $Cu_{12}Sb_4S_{13}$ is reported in some cases to have Cu excess up to 14 apfu (e.g. Skinner et al., 1972; Tatsuka and Morimoto, 1973; Lind and Makovicky, 1982; Makovicky and Karup-Møller, 1994). Unit-cell variation from 10.323 to 10.449 Å was reported for exsolved synthetic phases with compositions $\sim Cu_{12.3}Sb_4S_{13}$ and $\sim Cu_{13.8}Sb_4S_{13}$, respectively (Makovicky and Skinner, 1979). It should also be taken into account that Lind and Makovicky (1982) highlighted an analytical problem during electron microprobe analysis of synthetic tetrahedrite-group phases; indeed, those compositions having Cu > 12 apfu gave the same analytical results as those having

12 Cu apfu. This effect was noted for both Sb- and As-members of this sulfosalt group.

Nomenclature issues in Cu-rich tetrahedrite

Type material of tetrahedrite-(Cu) from Bankov (grain used for single-crystal study) has a chemical composition close to $Cu_{11.50}Zn_{0.30}Fe_{0.20}Sb_{4.00}S_{13} = {}^{M(2)}Cu_{6.00}{}^{M(1)}[Cu_4(Cu_{1.50}Zn_{0.30}Fe_{0.20})]$ ${}^{X(3)}Sb_4S_{13}$. Following Biagioni et al. (2020a), this chemistry can be idealised to the end-member formula $Cu_{10}^+Cu_2^{2+}Sb_4S_{13}$, assuming that formally divalent Cu^{2+} is the most abundant C constituent.

However, a majority of the chemical analyses of tetrahedrite-(Cu) and -(Fe) from Bankov (Figs. 4 and 5) are close to the ideal formula ${}^{M(2)}Cu_{6.00}{}^{M(1)}[Cu_4(Cu_{1.00}Fe_{1.00})]^{X(3)}Sb_4S_{13}$. This opens up a question of the valence of Fe. For the case with the presence of Fe^{3+}, applying the site-total-charge approach (Bosi et al., 2019) to this chemical composition, the end-member formula $Cu_6(Cu_5^+Fe^{3+})$ $Sb_4S_{13} = Cu_{11}Fe^{3+}Sb_4S_{13}$ is achieved. After initial examinations in the 1970s, the first detailed ^{57}Fe-Mössbauer studies were performed on Fe-bearing tetrahedrite in the 1990s (Charnock et al., 1989; Makovicky et al., 1990 and references herein), and completed by Nasonova et al. (2016) and Sobolev et al. (2017). Iron-bearing synthetic tennantite was studied by Makovicky et al. (2003). Though first studies confirm major Fe^{2+} towards the Fe pole, and major Fe^{3+} towards the Cu pole, examination of tennantite indicates the presence of Fe^{2+} down to 0.5 Fe apfu, as well as mixed valence Fe. Mixed valence iron seems to represent a substantial fraction of total iron at room T, owing to charge-transfer phenomena between Cu and Fe. For instance, at a content of 0.5 Fe apfu, Makovicky et al. (2003) estimated a formal valence ranging between +2.68 and +2.69 (+2.68 for sample 2052). The oxidation state of Cu was determined by Pattrick et al. (1993) and Gainov et al. (2008) on natural tetrahedrite and tennantite, and by Di Benedetto et al. (2005) on synthetic $Cu_{12}Sb_4S_{13}$. These three studies revealed the presence of divalent Cu in all Cu-rich samples. Nevertheless, while Di Benedetto et al. (2005) proposed two Cu^{2+} apfu, located at the Cu1 [= M(1)] site, Pattrick et al. (1993), confirmed by Gainov et al. (2008), indicates Cu^{2+} located at the Cu2 [= M(2)] triangular site, sometimes present for compositions excluding it according to the ionic model.
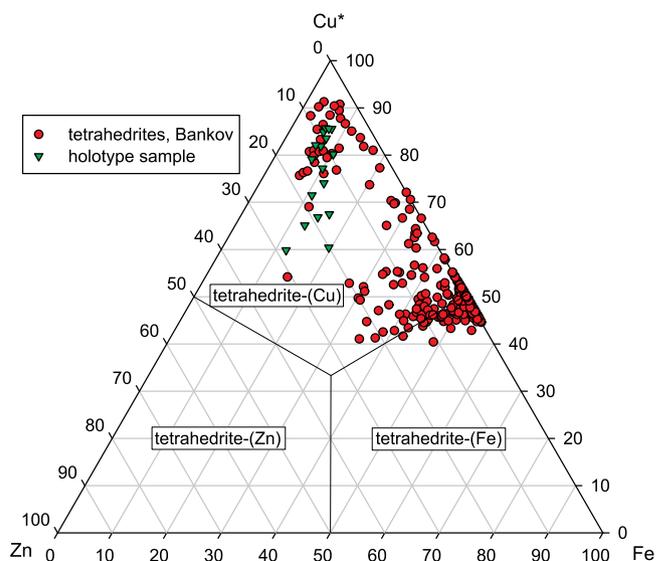

Figure 4. Chemical composition of tetrahedrite-(Cu) and tetrahedrite-(Fe) from Bankov in a ternary Fe–Cu*–Zn graph (at. units). Cu* = contents above 10 apfu.
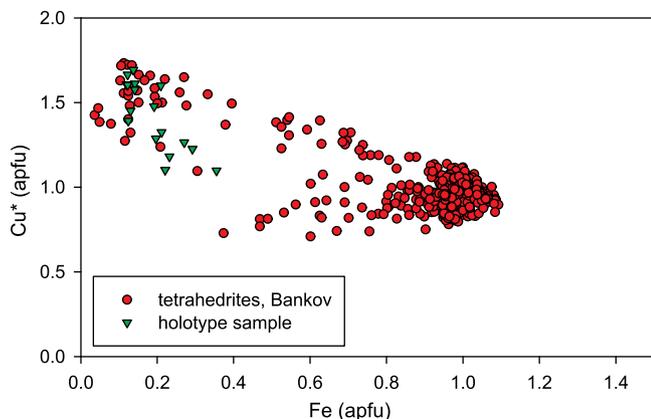
Figure 5. Chemical composition of tetrahedrite-(Cu) and tetrahedrite-(Fe) from Bankov in ternary Fe-Cu* graph (apfu). Cu* = contents above 10 apfu.

Moreover, in normal conditions, pure $Cu_{12}Sb_4S_{13}$ and $Cu_{12}Sb_4S_{13}$ are metallic (Lu and Morelli, 2013), that would correspond to partial replacement of Cu^{2+} by Cu^+ and one ligand hole (i.e. a mobile S electron).

Thus, the solid solution from the Fe-pole to the Cu-pole would ideally correspond to the following sequence ('ionic' model): (1) $Cu_{10}^+Fe_2^{2+} \rightarrow$ (2) $Cu_{10.5}^+Fe^{2+}Fe_{0.5}^{3+} \rightarrow$ (3) $Cu_{11}^+Fe^{3+} \rightarrow$ (4) $Cu_{10.5}^+Cu^{2+}Fe_{0.5}^{3+} \rightarrow$ (5) $Cu_{10}^+Cu_2^{2+}$. Compositions (1) to (3) correspond to the substitution rule $2Fe^{2+} \rightarrow Cu^+ + Fe^{3+}$, and compositions (3) to (5) to $Cu^+ + Fe^{3+} \rightarrow 2Cu^{2+}$. This sequence, controlled by an increase of f_{S_2}, indicates that iron oxidation precludes the appearance of formally divalent copper. According to nomenclature rules, one should distinguish three species: (i) 'tetrahedrite-(Fe^{2+})', from formula (1) up to formula (2); (ii) 'tetrahedrite-(Fe^{3+})', from formula (2) up to formula (4); and (iii) 'tetrahedrite-(Cu^{2+})', from formula (4) up to formula (5). This is in agreement with discussions by Biagioni *et al.* (2022) for the As-isotype tennantite-(Cu).

On this basis, the prevailing composition of tetrahedrite from the Bankov deposit (Figs 4 and 5) falls in the field of 'tetrahedrite-(Fe^{3+})'. Nevertheless, studies of natural and synthetic samples of tetrahedrite-(Cu) as well as tennantite-(Cu) through various physical methods revealed a very complex crystal chemistry, not completely understood up to now.

It thus appears that in Cu-rich tetrahedrite/tennantite one may have coexistence of Fe^{3+}, Fe^{2+}, Cu^{2+} and Cu^+ (with ligand hole). The distinction between the three species envisaged above on the basis of a simple ionic model is not pertinent, and it is more convenient for nomenclature purposes to consider only two species, tetrahedrite-(Fe) and tetrahedrite-(Cu). The same solution of nomenclature was published for the analogous pair tennantite-(Cu)/tennantite-(Fe) (Biagioni *et al.*, 2022).

Conclusion

The description of tetrahedrite-(Cu) adds further complexity to the tetrahedrite group, confirming on one side the structural plasticity of these chalcogenides, hosting several metals typical of hydrothermal settings, and on the other their role in recording the crystallisation conditions of ore assemblages.

In addition to improving the knowledge of ore mineralogy, the description of this new phase gives further information about the crystal chemistry of tetrahedrite-group minerals, with possible technological implications, as revealed by several recent studies

focusing on their high-tech properties (e.g. Suekuni *et al.*, 2014; Chetty *et al.*, 2015; Levinsky *et al.*, 2019; Rout *et al.*, 2023). Among the chemical compositions showing interesting properties, synthetic $Cu_{12}Sb_4S_{13}$ has potential electronic and photovoltaic properties and for this reason has been the focus of several research projects in the last decade (e.g. Tamilselvan and Bhattacharyya, 2018; Liu *et al.*, 2019, 2020; Long *et al.*, 2022; Mukherjee *et al.*, 2023; Lim *et al.*, 2024).

References

Andreasen J.W., Makovicky E., Lebech B. and Karup-Møller S. (2008) The role of iron in tetrahedrite and tennantite determined by Rietveld refinement of neutron powder diffraction data. *Physics and Chemistry of Minerals*, **35**, 447–454.

Biagioni C., George L.G., Cook N.J., Makovicky E., Moëlo Y., Pasero M., Sejkora J., Stanley C.J., Welch M.D. and Bosi F. (2020a) The tetrahedrite group: Nomenclature and classification. *American Mineralogist*, **105**, 109–122.

Biagioni C., Sejkora J., Musetti S., Velebil D. and Pasero M. (2020b) Tetrahedrite-(Hg), a new 'old' member of the tetrahedrite group. *Mineralogical Magazine*, **84**, 584–592.

Biagioni C., Sejkora J., Moëlo Y., Marcoux E., Mauro D. and Dolníček Z. (2022) Tennantite-(Cu), $Cu_{12}As_4S_{13}$, from Layo, Arequipa Department, Peru: a new addition to the tetrahedrite-group minerals. *Mineralogical Magazine*, **86**, 331–339.

Bosi F., Hatert F., Hålenius U., Pasero M., Miyawaki R. and Mills S.J. (2019) On the application of the IMA-CNMNC dominant-valency rule to complex mineral compositions. *Mineralogical Magazine*, **83**, 627–632.

Brese N.E. and O'Keeffe M. (1991) Bond-valence parameters for solids. *Acta Crystallographica*, **B47**, 192–197.

Cesbron F., Giraud R., Picot P. and Pillard F. (1985) La vinciennite, $Cu_{10}Fe_4Sn$ $(As,Sb)S_{16}$, une nouvelle espèce minérale. Etude paragénétique du gîte type de Chizeuil, Saône-et-Loire. *Bulletin de Minéralogie*, **108**, 447–456.

Charlat M. and Lévy C. (1975) Influence des principales substitutions sur le parametre cristallin de la série tennantite-tétraédrite. *Bulletin de la Société Française de Mineralogie et Cristallographie*, **98**, 152–158.

Charnock J.M., Garner C.D., Pattrick R.A.D. and Vaughan D.J. (1989) EXAFS and Mössbauer spectroscopic study of Fe-bearing tetrahedrites. *Mineralogical Magazine*, **53**, 193–199.

Chetty R., Bali A. and Mallik R.C. (2015) Tetrahedrites as thermoelectric materials: an overview. *Journal of Material Chemistry C*, **3**, 12364–12378.

Criddle A.J. and Stanley C.J. (1993) *Quantitative Data File for Ore Minerals*, third edition. Chapman & Hall, London.

Di Benedetto F., Bernardini G.P., Cipriani C., Emiliani C., Gatteschi D. and Romanelli M. (2005) The distribution of Cu(II) and the magnetic properties of the synthetic analogue of tetrahedrite: $Cu_{12}Sb_4S_{13}$. *Physics and Chemistry of Minerals*, **32**, 155–164.

Flack H.D. (1983) On enantiomorph-polarity estimation. *Acta Crystallographica*, **A39**, 876–881.

Gainov R.R., Dooglav A.V., Pn'kov I.N., Mukamedshin I.R., Savinkov A.V. and Mozgova N.N. (2008) Copper valence, structural separation and lattice dynamics in tennantite: NMR, NQR and SQUID studies. *Physics and Chemistry of Minerals*, **35**, 37–48.

George L.L., Cook N.J., and Ciobanu C.L. (2017) Minor and trace elements in natural tetrahedrite-tennantite: effects on element partitioning among base metal sulphides. *Minerals*, **7**, 17.

Grecula P., Abonyi A., Abonyiová M., Antaš J., Bartalský B., Bartalský J., Dianiška I., Ďuďa R., Gargulák M., Gazdačko Ľ., Hudáček J., Kobulský J., Lőrincz L., Macko J., Návesňák D., Németh Z., Novotný L., Radvanec M., Rojkovič I., Rozložník L., Varček C. and Zlocha Z. (1995) *Mineral deposits of the Slovak Ore Mountains, Vol 1*. Geocomplex, Bratislava, pp. 834 [in Slovak].

Haidinger W. (1845) Zweite Klasse: Geogenide. XIV. Ordnung, Glanze, I. Dystomglanz, Tetraedrit. Pp. 563–570 in: *Handbuch der Bestimmenden Mineralogie*, Bei Braumüller and Seidel, Wien.

Johnson M.L. and Burnham C.W. (1985) Crystal structure refinement of an arsenic-bearing argentian tetrahedrite. *American Mineralogist*, **70**, 165–170.

Johnson N.E., Craig J.R. and Rimstidt J.D. (1986) Compositional trends in tetrahedrite. *The Canadian Mineralogist*, **24**, 385–397.

Johnson N.E., Craig J.R. and Rimstidt J.D. (1987) Effect of substitutions on the cell dimension of tetrahedrite. *The Canadian Mineralogist*, **25**, 237–244.

Kraus W. and Nolze G. (1996) POWDER CELL – a program for the representation and manipulation of crystal structures and calculation of the resulting X-ray powder patterns. *Journal of Applied Crystallography*, **29**, 301–303.

Levinsky P., Candolfi C., Dauscher A., Tobola A., Hejtmánek J. and Lenoir B. (2019) Thermoelectric properties of the tetrahedrite−tennantite solid solutions $Cu_{12}Sb_{4-x}As_xS_{13}$ and $Cu_{10}Co_2Sb_{4-y}As_yS_{13}$ $(0 \leq x,y \leq 4)$. *Physical Chemistry Chemical Physics*, **21**, 4547–4555.

Lim K.H., Li M., Zhang Y., Wu Y., Zhou Q., Wang Q., Yang X., Liu P., Wang W., Wong K.W., Ng K.M., Liu Y. and Cabot A. (2024) Modulation doping of p-type $Cu_{12}Sb_4S_{13}$ toward improving thermoelectric performance. *Journal of Materials Science & Technology*, **171**, 71–79.

Lind I.L. and Makovicky E. (1982) Phase relations in the system Cu − Sb − S at 200°C, 108 Pa by hydrothermal synthesis. Microprobe analyses of tetrahedrite − a warning. *Neues Jahrbuch für Mineralogie, Abhandlungen*, **145**, 134–156.

Liu Y., Chen Q. Mei A., Hu B., Yang Z. and Chen W. (2019) Bandgap aligned $Cu_{12}Sb_4S_{13}$ quantum dots as efficient inorganic hole transport materials in planar perovskite solar cells with enhanced stability. *Sustainable Energy & Fuels*, **3**, 831–840.

Liu Y., Zhao X., Yang Z., Li Q., Wei W., Hu B. and Chen W. (2020) $Cu_{12}Sb_4S_{13}$ quantum dots with ligand exchange as hole transport materials in all-inorganic perovskite $CsPbI_3$ quantum dot solar cells. *ACS Applied Energy Materials*, **3**, 3521–3529.

Long C., Peng Z., Huang J., Wang Y., Luo W., Fu Y., Chen J. and Chen J. (2022) Enhancement on charge transfer properties of $Cu_{12}Sb_4S_{13}$ quantum dots hole transport materials by surface ligand modulation in perovskite solar cells. *New Journal of Chemistry*, **46**, 11751–11758.

Lu X. and Morelli D.T. (2013) Natural mineral tetrahedrite as a direct source of thermoelectric materials. *Physical Chemistry Chemical Physics*, **15**, 5762–5766.

Makovicky E. and Karup-Møller S. (1994) Exploratory studies on substitution of minor elements in synthetic tetrahedrite. Part I. Substitution by Fe, Zn, Co, Ni, Mn, Cr, V and Pb. Unit-cell parameter changes on substitution and the structural role of "Cu^{2+}". *Neues Jahrbuch für Mineralogie, Abhandlungen*, **167**, 89–123.

Makovicky E. and Skinner B.J. (1979) Studies of the sulfosalts of copper. VII. Crystal structures of the exsolution products $Cu_{12.3}Sb_4S_{13}$ and $Cu_{13.8}Sb_4S_{13}$ of unsubstituted synthetic tetrahedrite. *The Canadian Mineralogist*, **17**, 619–634.

Makovicky E., Forcher K., Lottermoser W. and Amthauer G. (1990) The role of Fe^{2+} and Fe^{3+} in synthetic Fe-substituted tetrahedrite. *Mineralogy and Petrology*, **43**, 73–91.

Makovicky E., Tippelt G., Forcher K., Lottermoser W., Karup-Møller S. and Amthauer G. (2003) Mössbauer study of Fe-bearing synthetic tennantite. *The Canadian Mineralogist*, **41**, 1125–1134.

Makovicky E., Karanović L., Poleti D., Balić-Žunić T. and Paar W.H. (2005) Crystal structure of copper-rich unsubstituted tennantite, $Cu_{12.5}As_4S_{13}$. *The Canadian Mineralogist*, **43**, 679–688.

Momma K., Shimizu M., Kusaba Y. and Ohki Y. (2022) Tetrahedrite-(Mn), IMA 2021-098. CNMNC Newsletter 65. *Mineralogical Magazine*, 86, 357, https://doi.org/10.1180/mgm.2022.14

Mukherjee S., Voneshen D.J., Duff A., Goddard P., Powell A.V. and Vaqueiro P. (2023) Beyond rattling: tetrahedrites as incipient ionic conductors. *Advanced Materials*, **35**, 2306088.

Nasonova D.I., Presniakov I.A., Sobolev A.V., Verchenko V.Yu., Tsirlin A.A., Wei Z., Dikarev E.V. and Shevelkov A.V. (2016) Role of iron in synthetic tetrahedrites revisited. *Journal of Solid State Chemistry*, **242**, 62–69.

Pattrick R.A.D., van der Laan G., Vaughan D.J. and Henderson C.M.B. (1993) Oxidation state and electronic configuration determination of copper in tetrahedrite group minerals by *L*-edge X-ray absorption spectroscopy. *Physics and Chemistry of Minerals*, **20**, 395–401.

Peterec D., Pauco M., Horský S. and Ďuďa R. (1990) A rare association of minerals from the Bankov magnesite deposit (Košice). *Zborník Východoslovenského múzea v Košiciach, Prírodné vedy*, **31**, 185–196.

Pfitzner A., Evain M. and Petříček V. (1997) $Cu_{12}Sb_4S_{13}$: A temperature-dependent structure investigation. *Acta Crystallographica Section B*, **53**, 337–345.

Pouchou J.L. and Pichoir F. (1985) "PAP" (ρZ) procedure for improved quantitative microanalysis. Pp. 104–106 in: *Microbeam Analysis* (J.T. Armstrong, editor). San Francisco Press, San Francisco.

Repstock A., Voudouris P. and Kolitsch U. (2015) New occurrences of watanabeite, colusite, "arsenosulvanite", and "Cu-excess" tetrahedrite-tennantite at the Pefka high-sulfidation epithermal deposit, northeastern Greece. *Neues Jahrbuch für Mineralogie, Abhandlungen*, **192**, 135–149.

Rout U., Tippireddy S., Kumari N., Dasgupta T. and Mallik R.C. (2023) Effect of Ag-addition on the thermoelectric properties of $Cu_{12}Sb_4S_{13}$ tetrahedrite. *Journal of Applied Physics*, **134**, 235102.

Sejkora J., Biagioni C., Vrtiška L. and Moëlo Y. (2021) Zvěstovite-(Zn), $Ag_6(Ag_4Zn_2)As_4S_{13}$, a new tetrahedrite-group mineral from Zvěstov, Czech Republic. *Mineralogical Magazine*, **85**, 716–724.

Sejkora J., Biagioni C., Števko M., Musetti S. and Peterec D. (2022) Tetrahedrite-(Cu), IMA 2022-078, in: CNMNC Newsletter 70. *Mineralogical Magazine*, **87**, 160–168, https://doi.org/10.1180/mgm.2022.135.

Sejkora J., Biagioni C., Škácha P., Musetti S., Kasatkin A.V. and Nestola F. (2023) Tetrahedrite-(Cd), $Cu_6(Cu_4Cd_2)Sb_4S_{13}$, from Radětice near Příbram, Czech Republic: the new Cd-member of tetrahedrite-group. *European Journal of Mineralogy*, **35**, 897–907.

Sheldrick G.M. (2015) Crystal structure refinement with SHELXL. *Acta Crystallographica*, **C71**, 3–8.

Skinner B.J., Luce F.D. and Makovicky E. (1972) Studies of the sulfosalts of copper III. Phases and phase relations in the system Cu–Sb–S. *Economic Geology*, **67**, 924–938.

Sobolev A.V., Presniakov I.A., Nasonova D.I., Verchenko V.Yu. and Shevelkov A.V. (2017) Thermally activated electron exchange in $Cu_{12-x}Fe_xSb_4S_{13}$ (x = 1.3, 1.5) tetrahedrites: A Mössbauer study. *Journal of Physical Chemistry*, **121**, 4548–4557.

Suekuni K., Tomizawa Y., Ozaki T. and Koyano M. (2014) Systematic study of electronic and magnetic properties for $Cu_{12-x}TM_xSb_4S_{13}$ (TM= Mn, Fe, Co, Ni, and Zn) tetrahedrite. *Journal of Applied Physics*, **115**, 143702.

Tamilselvan M. and Bhattacharyya A. J. (2018) Tetrahedrite ($Cu_{12}Sb_4S_{13}$) ternary inorganic hole conductor for ambient processed stable perovskite solar cells. *ACS Applied Energy Materials*, **1**, 4227–4234.

Tatsuka K. and Morimoto N. (1973) Composition variation and polymorphism of tetrahedrite in the Cu-Sb-S system below 400° C. *American Mineralogist*, **58**, 425–434.

Voudouris P., Repstock A., Spry P.G., Frenzel M., Mavrogonatos C., Keith M., Tarantola A., Melfos V., Tombros S., Zhai D., Cook N.J., Ciobanu C.L., Schaarschmidt A., Rieck B., Kolitsch U. and Falkenberg J.J. (2022) Physicochemical constraints on indium-, tin-, germanium-, gallium-, gold-, and tellurium-bearing mineralizations in the Pefka and St Philippos polymetallic vein- and breccia-type deposits, Greece. *Ore Geology Reviews*, **140**, 104348.

Wang Y., Chen R., Gu X., Nestola F., Hou Z., Yang Z., Dong G., Guo H. and Qu K. (2023) Tetrahedrite-(Ni), $Cu_6(Cu_4Ni_2)Sb_4S_{13}$, the first nickel member

of tetrahedrite group mineral from Luobusa chromite deposits, Tibet, China. *American Mineralogist*, **108**(10), 1984–1992.

Warr L.N. (2021) IMA-CNMNC approved mineral symbols. *Mineralogical Magazine*, **85**, 291–320.

Welch M.D., Stanley C.J., Spratt J. and Mills S.J. (2018) Rozhdestvenskayaite $Ag_{10}Zn_2Sb_4S_{13}$ and argentotetrahedrite $Ag_6Cu_4(Fe^{2+},Zn)_2Sb_4S_{13}$: two Ag-dominant members of the tetrahedrite group. *European Journal of Mineralogy*, **30**, 1163–1172.

Wilson A.J.C. (editor) (1992) *International Tables for Crystallography Volume C: Mathematical, Physical and Chemical Tables.* Kluwer Academic Publishers, Dordrecht, The Netherlands.

Wuensch B.J. (1964) The crystal structure of tetrahedrite, $Cu_{12}Sb_4S_{13}$. *Zeitschrift für Kristallographie*, **119**, 437–453.

Wuensch B.J., Takéuchi Y. and Nowacki W. (1966) Refinement of the crystal structure of binnite, $Cu_{12}As_4S_{13}$. *Zeitschrift für Kristallographie*, **123**, 1–20.